

# Migration Tendencies of Group 14 Element Ligands in the Coordination Sphere of Cationic Phosphenium Iron Complexes

C. H. Suresh and Nobuaki Koga\*

Graduate School of Human Informatics, Nagoya University,  
Chikusa-ku, Nagoya, 464-8601, Japan

Received May 16, 2001

Structural and bonding features of the model iron–phosphenium cation complexes of the type  $[\text{Cp}(\text{CO})(\text{EH}_2\text{R})\text{FePNHCH}_2\text{CH}_2\text{NH}]^+$  ( $\text{E}$  = group 14 element;  $\text{R}$  =  $\text{H}$  and  $\text{CH}_3$ ) as well as the migration of the  $\text{EH}_2\text{R}$  group from iron to phosphorus (1,2-migration) and that of a  $\text{CH}_3$  group from  $\text{E}$  to phosphorus (1,3-migration) have been studied using the hybrid DFT-B3LYP method. The remarkable stability of these complexes is due to the conjugation around  $\text{P}$ , which can be partitioned into  $\text{N}-\text{P}^+-\text{N}$  lone pair  $\pi$ -conjugation and the  $\text{Fe}-\text{P}^+$   $\pi$  bond. Both together contribute 61.9 kcal/mol to its stability. The calculations suggest that all the 1,2-migrations are feasible reactions and the  $\text{CH}_2\text{R}$  migration has the highest tendency because of its small activation barrier (1.3 kcal/mol) and the exothermicity. However, the charge distribution on the structures involved in these reactions points out that external factors such as solvent and the counteranion can greatly influence the courses of the reactions. Compared to the 1,2-migrations, the 1,3-migrations of a methyl group from  $\text{C}$ ,  $\text{Si}$ , and  $\text{Sn}$  need much higher activation energies (51.7, 42.7, and 32.7 kcal/mol, respectively), and all are endothermic. A rationalization for the reaction energies and the activation barriers is obtained by bond strength analysis. The bond strengths obtained in this study for  $\text{C}-\text{C}$ ,  $\text{C}-\text{Si}$ ,  $\text{C}-\text{Sn}$ ,  $\text{P}-\text{C}$ ,  $\text{P}-\text{Si}$ ,  $\text{P}-\text{Sn}$ ,  $\text{Fe}-\text{C}$ ,  $\text{Fe}-\text{Si}$ ,  $\text{Fe}-\text{Sn}$ ,  $\text{Fe}=\text{C}$ ,  $\text{Fe}=\text{Si}$ , and  $\text{Fe}=\text{Sn}$  are 90.4, 86.6, 69.6, 93.7, 81.4, 72.1, 31.8, 41.7, 36.3, 77.4, 82.3, and 69.9 kcal/mol, respectively. Further, in the presence of a water molecule as a model base the 1,3-methyl migrations from  $\text{Si}$  to  $\text{P}$  and  $\text{Sn}$  to  $\text{P}$  become exothermic, and their activation barriers were lowered to a significant amount. An explanation for this behavior is given based on the Fisher-type and Schrock-type metal–ligand double-bond formation in these complexes. When  $\text{E} = \text{Sn}$  and  $\text{R} = \text{CH}_3$ , a realistic base molecule could favor the 1,3-migration over the 1,2-migration, consistent with the experimental facts.

## Introduction

Organotransition metal complexes are well known for their diverse and interesting chemical transformations (substance transformation reactions) and catalytic activity.<sup>1,2</sup> Migration reactions are one of the most closely examined substance transformation reactions in the recent years.<sup>3,4</sup> For instance, one can find in the recent literature of transition metal chemistry titles containing wording such as “metal-to-ring alkyl migration”,<sup>3a</sup> “methyl-to-double-bond migration”,<sup>3b</sup> “metal-to-metal silyl migration”,<sup>3c</sup> “alkyl migration”,<sup>3d,e</sup> “hydrogen migration”,<sup>3f</sup> “hydride migration”,<sup>3g</sup> “unusual silyl migration”,<sup>3h,i</sup> “migratory insertion”,<sup>3j</sup> “migration reaction of a hyper-

valent fragment”,<sup>3k</sup> “oxygen-to-iron methyl migration”,<sup>3l</sup> “reversible migration”,<sup>3m,n</sup> etc. It is well known that migratory insertion reactions such as olefin and carbonyl insertions are key elementary reactions. For example, complexes of the type  $\text{L}_n\text{M}(=\text{SiR}_2)\text{SiR}_3$  cata-

(1) (a) Collman, J. P.; Hegedus, L. S.; Norton, J. R.; Finke, R. G. *Principles and Applications of Organotransition Metal Chemistry*; University Science Books: Mill Valley, CA, 1987. (b) Curtis, M. D.; Epstein, P. S. *Adv. Organomet. Chem.* **1981**, *19*, 213. (c) Pannel, K. H.; Rozell, J. M., Jr.; Hernandez, C. *J. Am. Chem. Soc.* **1989**, *111*, 4482. (d) Shama, H. K.; Pannel, K. H. *Chem. Rev.* **1995**, *95*, 1351. (e) Schubert, U. *Angew. Chem., Int. Ed. Engl.* **1994**, *33*, 419.

(2) (a) Haynes, A.; George, M. W.; Haward, M. T.; Poliakov, M.; Turner, J. J.; Boag, N. M.; Green, M. J. *Am. Chem. Soc.* **1991**, *113*, 2011. (b) Mitchell, G. P.; Tilley, T. D. *Organometallics* **1998**, *17*, 2912. (c) Tamao, K.; Sun, G. -R.; Kawachi, A. *J. Am. Chem. Soc.* **1995**, *117*, 8043. (d) Braunstein, P.; Faure, T.; Knorr, M. *Organometallics* **1999**, *18*, 1791.

(3) (a) Carpenter, N. F.; Khan, M. A.; Nicholas, K. M. *Organometallics* **1999**, *18*, 1569. (b) Vignalok, A.; Milstein, D. *Organometallics* **2000**, *19*, 2341. (c) Shelby, Q. D.; Lin, W.; Girolami, G. S. *Organometallics* **1999**, *18*, 1904. (d) Nakazawa, H.; Yamaguchi, Y.; Miyoshi, K. *Organometallics* **1996**, *15*, 1337. (e) Hughes, R. P.; Trujillo, H. A.; Egan, J. W., Jr.; Rheingold, A. L. *J. Am. Chem. Soc.* **2000**, *122*, 2261. (f) Doherty, S.; Hogarth, G.; Waugh, M.; Clegg, W.; Elsegood, M. R. *J. Organometallics* **2000**, *19*, 4557. (g) Amor, F.; Jesús, E. d.; Royo, P.; Miguel, A. V. d. *Inorg. Chem.* **1996**, *35*, 3440. (h) Chen, T.; Wu, Z.; Li, L.; Sorasaene, K. R.; Diminnie, J. B.; Pan, H.; Guzei, I. A.; Rheingold, A. L.; Xue, Z. *J. Am. Chem. Soc.* **1998**, *120*, 13519. (i) Huang, D.; Folting, K.; Caulton, K. G. *J. Am. Chem. Soc.* **1999**, *121*, 10318. (j) Antwi-Nasiah, F. H.; Oke, O.; Cowie, M. *Organometallics* **1996**, *15*, 1042. (k) Kubo, K.; Nakazawa, H.; Kawamura, K.; Mizuta, T.; Miyoshi, K. *J. Am. Chem. Soc.* **1998**, *120*, 6715. (l) Luo, W.; Fong, R. H.; Hersh, W. H. *Organometallics* **1997**, *16*, 4192. (m) Albrecht, M.; Gossage, R. A.; Spek, A. L.; Koten, G. v. *J. Am. Chem. Soc.* **1999**, *121*, 11898. (n) Rickard, C. E. F.; Roper, W.; Woodman, T. J.; Wright, L. J. *Chem. Commun.* **1999**, 1101.

(4) See also: (a) Braunstein, P.; Knorr, M.; Stern, C. *Coord. Chem. Rev.* **1998**, *178–180*, 903. (b) Axe, F. U.; Marynick, D. S. *Organometallics*, **1987**, *6*, 572. (c) Fischer, H.; Scheck, P. A. *Chem. Commun.* **1999**, 1031. (d) Liu, L.-K.; Chang, K.-Y.; Wen, Y.-S. *J. Chem. Soc., Dalton Trans.* **1998**, 741. (e) Cammell, E. J.; Andersen, J.-A. M. *J. Organomet. Chem.* **2000**, *604*, 7.

lyze the redistribution of substituents on silicon atoms.<sup>5</sup> The mechanism involved in this reaction is the intramolecular 1,3-substituent migration from the silyl group to the silylene ligand in the silyl(silylene) complex. Recently, Nakazawa et al.<sup>6</sup> have reported convincing evidence for the intramolecular 1,2-migration of group 14 element ligands as well as the 1,3-migration of a ligand substituent in iron complexes of the type

$\text{Cp}(\text{CO})(\text{ER}_3)\text{Fe}\{\text{P}(\text{OCH}_3)\text{N}(\text{CH}_3)\text{CH}_2\text{CH}_2\text{NCH}_3\}$  (E = C, Si, Ge, and Sn; R = H when E = C, otherwise R = CH<sub>3</sub>). Interestingly, these reactions showed a strong dependency on the nature of the group 14 element that is attached to the iron atom. When E = C, a phosphonium cation given by methoxy dissociation rapidly undergoes migratory insertion of the phosphonium ligand into the Fe–C bond (i.e., 1,2-migration of Me from Fe to P). However, with E = Si and Ge, only stable cationic phosphonium complexes are formed. In contrast to these, when E = Sn, a stannylyene complex is formed by the methyl migration from Sn to P (1,3-migration). The existence of base-stabilized and base-free stannylyene complexes was also identified in the 1,3-migrations. In fact, these reactions can be considered as one of the most interesting migration reactions that occur in the coordination sphere of a metal atom. A careful theoretical study is needed to understand the reasons behind the different outcomes of such apparently similar reactions, and that is the subject of the present paper.

A cationic phosphonium ligand  $[\text{PX}_2]^+$  is electronically similar to much familiar carbene and silylene ligands since all of them can act as a  $\sigma$ -donor as well as a  $\pi$ -acceptor due to the availability of lone pair electrons and a vacant valence shell p orbital on them.<sup>7</sup> The reactions reported in the previous paragraph<sup>5,6</sup> are characterized by the presence of either a silylene or a cationic phosphonium ligand. The presence of a vacant p orbital in these ligands is often considered as the driving force for the migration reactions. Phosphonium cations have been studied as a new class of  $\pi$ -acceptor ligands for rhodium-catalyzed hydroformylation of styrene.<sup>9</sup> Synthesis of new chiral as well as aromatic phosphonium cations have recently appeared in the literature.<sup>10,11</sup>

It has been observed in many contexts that when X = NR<sub>2</sub> group, the phosphonium cation possesses considerable stability.<sup>7,11–13</sup> In fact, almost all the reported phosphonium cations possess at least one P–N bond.<sup>7–15</sup>

(5) (a) Ueno, K.; Sakai, M.; Ogino, H. *Organometallics* **1998**, *17*, 2138. (b) Ueno, K.; Nakano, K.; Ogino, H. *Chem. Lett.* **1996**, 459. (c) Tobita, H.; Ueno, K.; Ogino, H. *Bull. Chem. Soc. Jpn.* **1988**, *61*, 27974.

(6) Nakazawa, H.; Yamaguchi, Y.; Kawamura, K.; Miyoshi, K. *Organometallics* **1997**, *16*, 4626.

(7) Cowley, A. H.; Kemp, R. A. *Chem. Rev.* **1985**, *85*, 367.

(8) Breit, B. *J. Mol. Catal. A: Chem.* **1999**, *143*, 143.

(9) Brunel, J.-M.; Villard, R.; Buono, G. *Tetrahedron Lett.* **1999**, *40*, 4669.

(10) Denk, M. K.; Gupta, S.; Ramachandran, R. *Tetrahedron Lett.* **1996**, *37*, 9025.

(11) (a) Cowley, A. H.; Cushner, M. C.; Lattman, M.; McKee, M. L.; Szobota, J. S.; Wilburn, J. C. *Pure Appl. Chem.* **1980**, *52*, 789. (b) Cowley, A. H.; Kemp, R. A. *Chem. Rev.* **1985**, *85*, 367. (c) Cowley, A. H.; Stewart, M. C.; Szobota, J. S. *J. Am. Chem. Soc.* **1978**, *100*, 7784.

(12) (a) Friedrich, P.; Huttner, G.; Luber, J.; Schmidpeter, A. *Chem. Ber.* **1978**, *111*, 1558. (b) Kopp, R. W.; Bond, A. C.; Parry, R. W. *Inorg. Chem.* **1976**, *15*, 3042. (c) Burford, N.; Royan, B. W.; Linden, A.; Cameron, T. S. *Inorg. Chem.* **1989**, *28*, 144.

(13) (a) Gamon, N.; Reichardt, C. *Angew. Chem., Int. Ed. Engl.* **1977**, *16*, 404. (b) Jungermann, E.; McBride, J. J.; Clutter, R.; Mais, A. *J. Org. Chem.* **1962**, *27*, 606.

The stability together with the  $\sigma$ -donor and  $\pi$ -acceptor character ensures a great variety of reactivity as well as rich coordination chemistry to these species.<sup>14–21</sup> The present authors have recently proved that the stability of a  $[\text{P}(\text{NR}_2)_2]^+$  type cation is due to the conjugation involving the nitrogen lone pair electrons and the vacant valence shell p orbital on the phosphorus atom,<sup>22</sup> which is named lone pair  $\pi$ -conjugation. For example, in  $[\text{P}(\text{NH}_2)_2]^+$  the N–P<sup>+</sup>–N lone pair  $\pi$ -conjugation contributes 68.1 kcal/mol toward its stabilization. Geometrical evidence for this type of conjugation is the considerable shortening of the P–N bonds.<sup>22</sup> In the case of  $[\text{P}(\text{NH}_2)_2]^+$ , the P–N bond shortening as compared to a typical P–N single bond is around 0.1 Å. The above-discussed features can be clearly understood from the molecular orbitals of the  $[\text{P}(\text{NH}_2)_2]^+$  cation as depicted in Figure 1.

In this paper using the hybrid density functional theory method we studied the model reactions of the cationic phosphonium complexes shown in Scheme 1: the 1,2-migration of an EH<sub>2</sub>R group (R = H and CH<sub>3</sub>; E = C, Si, and Sn) from Fe to P and the 1,3-migration of a methyl group from E to P. The phosphonium cation selected in the model complex is  $[\text{PNHCH}_2\text{CH}_2\text{NH}]^+$ . The stability and reactivity of these complexes will be analyzed on the basis of their structural, energetic, and electronic properties, and the results on the mechanisms will be compared with the experiments reported by Nakazawa et al.,<sup>6</sup> in order to elucidate the origin of the different outcomes of similar reactions among the E atoms.

## Computational Methods

All the calculations were performed by using the Gaussian98 set of programs.<sup>23</sup> Throughout the calculations, first, the geometry optimizations have been done at the B3LYP/LANL2DZ level of density functional theory (DFT),<sup>24</sup> and then the vibrational frequency calculations have been carried out to characterize the structures thus determined. LANL2DZ stands for the Los Alamos effective core potentials (ECP) plus split-valence basis functions.<sup>25</sup> In this basis set, provision is given for the use of ECP replacing the core electrons. The

(14) (a) Brunel, J.-M.; Villard, R.; Buono, G. *Tetrahedron Lett.* **1999**, *40*, 4669. (b) Denk, M. K.; Gupta, S.; Ramachandran, R. *Tetrahedron Lett.* **1996**, *37*, 9025. (c) Zhang, C.-J.; Zhan, C.-G.; Huang, T.-B. *J. Mol. Struct. (THEOCHEM)* **1995**, *357*, 9.

(15) (a) Breit, B. *J. Mol. Catal.* **1999**, *143*, 143. (b) Reisacher, H.-U.; Duesler, E. N.; Paine, R. T. *J. Organomet. Chem.* **1998**, *564*, 13. (c) Malisch, W.; Hirth, U.-A.; Grün, K.; Schmeusser, M. *J. Organomet. Chem.* **1999**, *572*, 207. (d) Montemayar, R. G.; Sauer, D. T.; Fleming, S.; Bennett, D. W.; Thomas, M. G.; Parry, R. W. *J. Am. Chem. Soc.* **1978**, *100*, 2231.

(16) (a) Snow, S. S.; Jiang, D.-X.; Parry, R. W. *Inorg. Chem.* **1987**, *26*, 1629. (b) Luber, J.; Schmidpeter, A. *J. Chem. Soc., Chem. Commun.* **1976**, 887. (c) Luber, J.; Schmidpeter, A. *Angew. Chem., Int. Ed. Engl.* **1976**, *15*, 111.

(17) (a) Burford, N.; Dipchand, A. I.; Royan, B. W.; White, P. S. *Inorg. Chem.* **1990**, *29*, 4938. (b) Burford, N.; Losier, P.; McDonald, C.; Kyrimis, V.; Bakshi, P. K.; Cameron, T. S. *Inorg. Chem.* **1994**, *33*, 1434. (18) Choi, H. W.; Gavin, R. M.; Muetterties, E. L. *J. Chem. Soc., Chem. Commun.* **1979**, 1085.

(19) Cowley, A. H.; Kemp, R. A.; Ebsworth, E. A. V.; Rankin, D. W. H.; Walkinshaw, M. D. *J. Organomet. Chem.* **1984**, *265*, C19.

(20) (a) Nakazawa, H.; Ohta, M.; Yoneda, H. *Inorg. Chem.* **1988**, *27*, 973. (b) Nakazawa, H.; Yamaguchi, Y.; Miyoshi, K. *J. Organomet. Chem.* **1994**, *465*, 193. (c) Nakazawa, H.; Yamaguchi, Y.; Mizuta, T.; Miyoshi, K. *Organometallics* **1995**, *14*, 4173.

(21) (a) Mizuta, T.; Yamasaki, T.; Nakazawa, H.; Miyoshi, K. *Organometallics* **1996**, *15*, 1093. (b) Nakazawa, H.; Yamaguchi, Y.; Miyoshi, K. *Organometallics* **1996**, *15*, 4661.

(22) Suresh, C. H.; Koga, N. *Inorg. Chem.* **2000**, *39*, 3718.

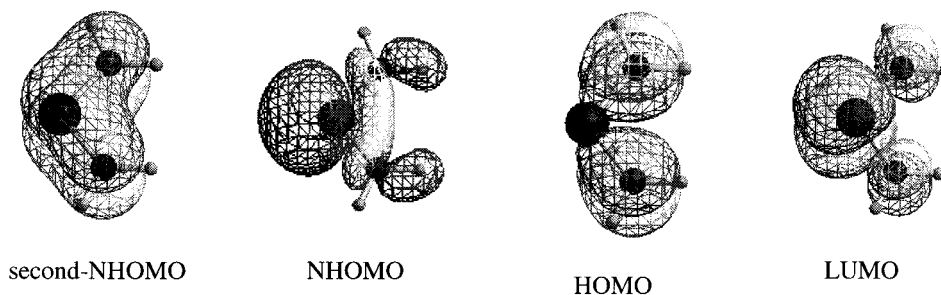
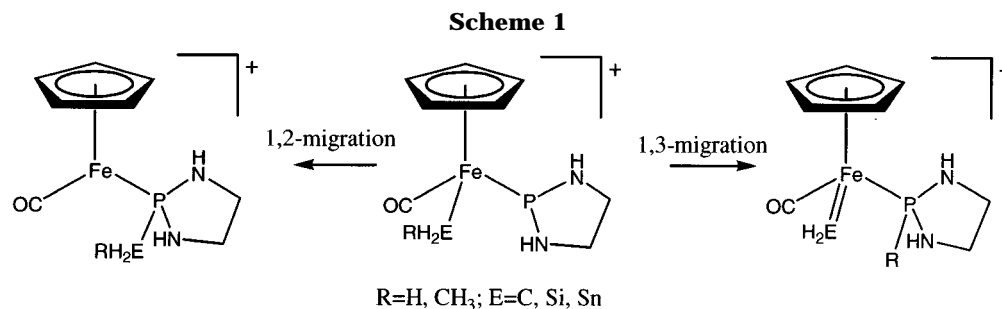


**Figure 1.** Some molecular orbitals of phosphonium cation  $[P(NH_2)_2]^+$ .



structures were further optimized with adding polarization functions for P, Si, and Sn to the basis set, starting from the B3LYP/LANL2DZ structures. We call this larger basis set LANL2DZ+pol.

## Results and Discussion

### 1,2-Migration of $EH_3$ Groups (E = C, Si, and Sn).

The optimized structures for  $CH_3$  1,2-migration and those for  $SiH_3$  1,2-migration determined at the B3LYP/LANL2DZ+pol level are shown in Figures 2 and 3, respectively, in which the potential energy profiles are shown as well. The selected bond distances of the stationary points are summarized in Table 1 for all the  $EH_3$  1,2-migrations we studied.

The P–N bond distances in the reactants obtained at the B3LYP/LANL2DZ level are all in the range 1.695–1.707 Å, which is much longer than the experimental bond distances<sup>6</sup> of 1.601–1.621 Å in  $Cp(CO)(Si(CH_3)_3)Fe\{PN(CH_3)CH_2CH_2NCH_3\}^+$ . However, the B3LYP/LANL2DZ+pol level calculation shortens the P–N bond distances into the range 1.662–1.665 Å, which are closer to the experimental distances. Therefore, hereafter, the results at the B3LYP/LANL2DZ+pol level will be used for the entire discussion unless otherwise noted.

### (a) Geometric Features of Reactants and Products.

All the reactant cationic complexes possess an 18-electron configuration. The calculations showed that these species have a piano stool structure and that the  $PNHCCNH$  skeleton possesses a near planar structure. These geometrical features are in very good agreement with those obtained in the crystal structure<sup>6</sup> of the complex  $Cp(CO)(Si(CH_3)_3)Fe\{PN(CH_3)CH_2CH_2NCH_3\}^+$ . The planarity of the  $PNHCCNH$  skeleton as well as the short P–N bonds indicates the conjugation of the nitrogen lone pair electrons with the vacant p orbital on the P atom, as shown in the Introduction. In Figure 4, some important localized Kohn–Sham orbitals (LKSO) are depicted that represent the Fe–P and P–N bonds (localization procedure gave four bent localized orbitals over the two P–N bonds; by transforming them we obtained the  $\pi$  orbitals, LKSO-2 and LKSO-3, shown in Figure 4 and the two P–N  $\sigma$  bond orbitals). LKSO-1 represents the coordination of the lone pair on the P atom to the Fe atom, which is mainly the interaction between NHOMO in Figure 1 and the vacant  $d_{\sigma}$  orbital of the Fe atom. LKSO-2 is the bonding  $\pi$  orbital showing the N–P<sup>+</sup>–N lone pair conjugation, and LKSO-3 is a nonbonding orbital. These two orbitals are similar to the NHOMO and second NHOMO of the phosphonium cation shown in Figure 1, and they do not participate in the interaction with the Fe atom. On the other hand, the LKSO-4 clearly shows that the occupied d orbital of the Fe atom conducts the  $\pi$  interaction mainly with the LUMO of the  $[PNHCH_2CH_2NH]^+$  ligand in Figure 1. In other words coordination of the phosphonium cation to the Fe moiety leads to extension of the lone pair  $\pi$  conjugation to the Fe atom as schematically drawn in Figure 5.

As compared to the reactants, the four main changes are thus observed in the products: (i) formation of a P–E bond at the expense of an Fe–E bond, (ii) formation of a coordinated Fe–N bond, (iii) lengthening of the

(23) Frisch, M. J.; Trucks, G. W.; Schlegel, H. B.; Scuseria, G. E.; Robb, M. A.; Cheeseman, J. R.; Zakrzewski, V. G.; Montgomery, Jr., J. A.; Stratmann, R. E.; Burant, J. C.; Dapprich, S.; Millam, J. M.; Daniels, A. D.; Kudin, K. N.; Strain, M. C.; Farkas, O.; Tomasi, J.; Barone, V.; Cossi, M.; Cammi, R.; Mennucci, B.; Pomelli, C.; Adamo, C.; Clifford, S.; Ochterski, J.; Petersson, G. A.; Ayala, P. Y.; Cui, Q.; Morokuma, K.; Malick, D. K.; Rabuck, A. D.; Raghavachari, K.; Foresman, J. B.; Cioslowski, J.; Ortiz, J. V.; Stefanov, B. B.; Liu, G.; Liashenko, A.; Piskorz, P.; Komaromi, I.; Gomperts, R.; Martin, R. L.; Fox, D. J.; Keith, T.; Al-Laham, M. A.; Peng, C. Y.; Nanayakkara, A.; Gonzalez, C.; Challacombe, M.; Gill, P. M. W.; Johnson, B.; Chen, W.; Wong, M. W.; Andres, J. L.; Gonzalez, C.; Head-Gordon, M.; Replogle, E. S.; Pople, J. A. *Gaussian 98*, Revision A.3; Gaussian, Inc.: Pittsburgh, PA, 1998.

(24) (a) Becke, A. D. *J. Chem. Phys.* **1993**, *98*, 1372. (b) Becke, A. D. *J. Chem. Phys.* **1993**, *96*, 5648.

(25) (a) Hay, P. J.; Wadt, W. R. *J. Chem. Phys.* **1985**, *82*, 275. (b) Wadt, W. R.; Hay, P. J. *J. Chem. Phys.* **1985**, *82*, 284. (c) Hay, P. J.; Wadt, W. R. *J. Chem. Phys.* **1985**, *82*, 299.

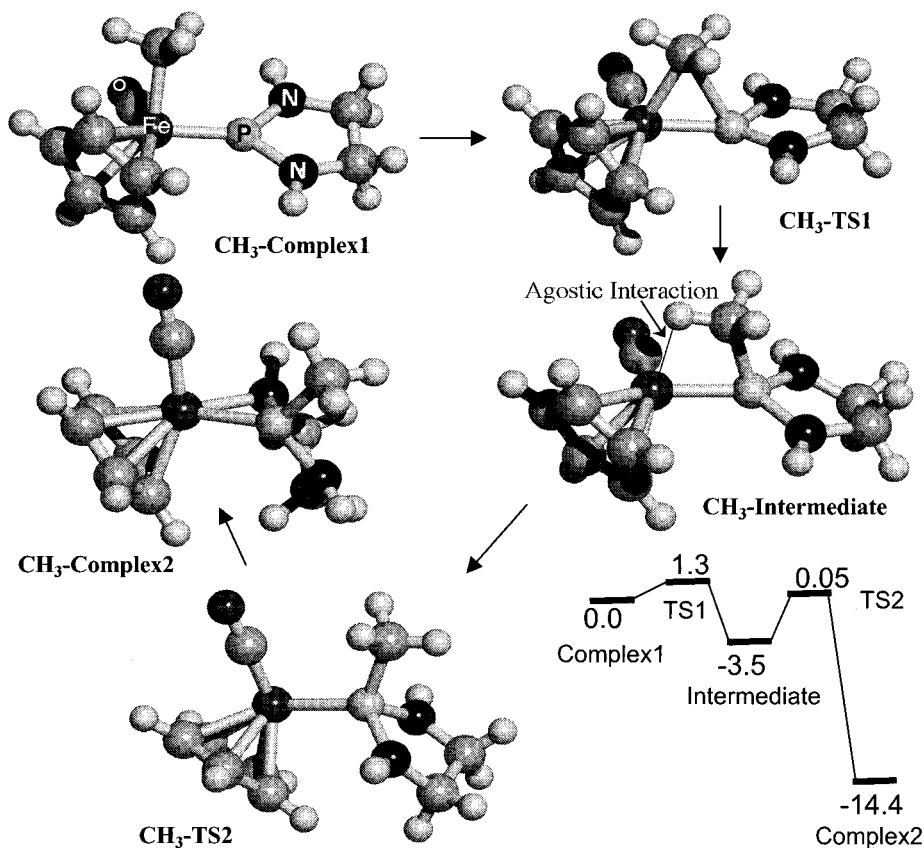


**Figure 2.** Optimized structures for the 1,2-migration of the  $\text{CH}_3$  group in the coordination sphere of iron and the corresponding energy level diagram in kcal/mol. C and H atoms are not labeled.

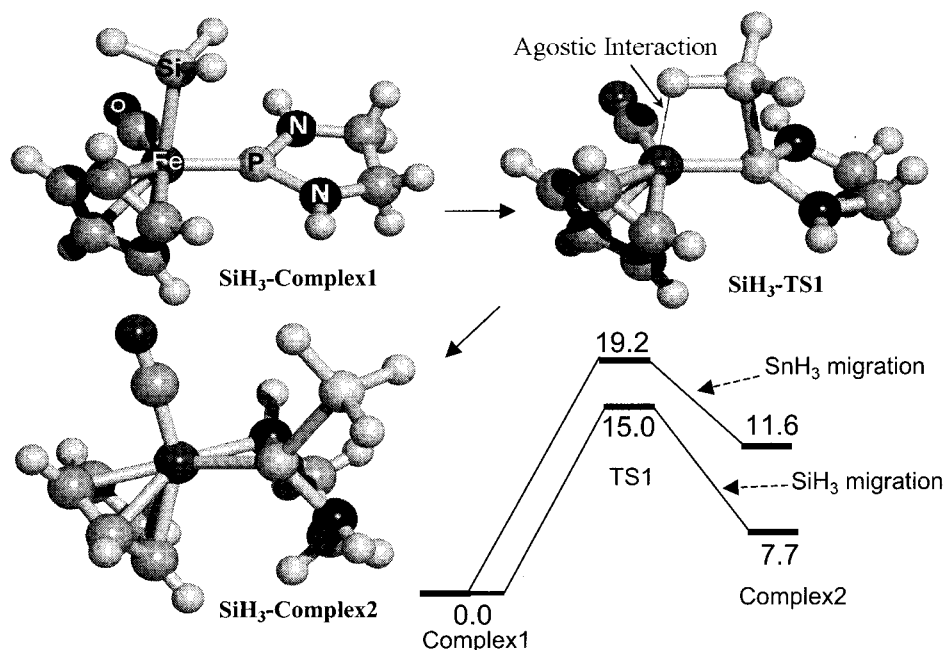


**Figure 3.** Optimized structures for the 1,2-migration of the  $\text{SiH}_3$  group in the coordination sphere of iron. Also shown is the energy level diagram for the 1,2-migrations of  $\text{SiH}_3$  and  $\text{SnH}_3$  groups in kcal/mol. C and H atoms are not labeled.

$\text{Fe-P}$  bond by 0.127–0.155 Å, and (iv) lengthening of the  $\text{P-N}$  bonds by 0.039–0.135 Å. The lengthening of the  $\text{P-N}$  and  $\text{Fe-P}$  bonds, (iii) and (iv), is ascribed to the breaking of the  $\pi$ -conjugation shown in Figure 5, which is caused by the  $\text{P-E}$  bond formation.

As shown in Figures 2 and 3, the 1,2-migration of the  $\text{CH}_3$  group is 14.4 kcal/mol exothermic, whereas those of the  $\text{SiH}_3$  and  $\text{SnH}_3$  groups are 7.7 and 11.6 kcal/mol endothermic. This difference in the energy of reactions will be discussed later.

**Table 1. Important Bond Length Parameters (in Å) in 1,2-Migrations of CH<sub>3</sub>, SiH<sub>3</sub>, and SnH<sub>3</sub> Groups<sup>a</sup>**

B3LYP/LanL2DZ+pol	Fe–P	Fe–E	P–E	P–N1	P–N2	Fe–N1
CH <sub>3</sub> –Complex1	2.067	2.072	no bond	1.662	1.665	no bond
CH <sub>3</sub> –TS1	2.059	2.174	2.372	1.664	1.663	no bond
CH <sub>3</sub> –Intermediate	2.136	2.444	1.912	1.688	1.681	no bond
CH <sub>3</sub> –TS2	2.286	no bond	1.855	1.702	1.703	no bond
CH <sub>3</sub> –Complex2	2.194	no bond	1.845	1.782	1.704	2.097
SiH <sub>3</sub> –Complex1	2.058	2.378	no bond	1.663	1.665	no bond
SiH <sub>3</sub> –TS1	2.114	2.690	2.424	1.686	1.684	no bond
SiH <sub>3</sub> –Complex2	2.209	no bond	2.320	1.795	1.714	2.078
SnH <sub>3</sub> –Complex1	2.058	2.638	no bond	1.665	1.667	no bond
SnH <sub>3</sub> –TS1	2.136	2.936	2.681	1.690	1.690	no bond
SnH <sub>3</sub> –Complex2	2.213	no bond	2.625	1.800	1.718	2.074

<sup>a</sup> Very similar bond length parameters are obtained for 1,2-migrations of CH<sub>2</sub>CH<sub>3</sub>, SiH<sub>2</sub>CH<sub>3</sub>, and SnH<sub>2</sub>CH<sub>3</sub>. See Supporting Information. Nitrogen atom nearer to the carbonyl group is designated as N1 and the other as N2.

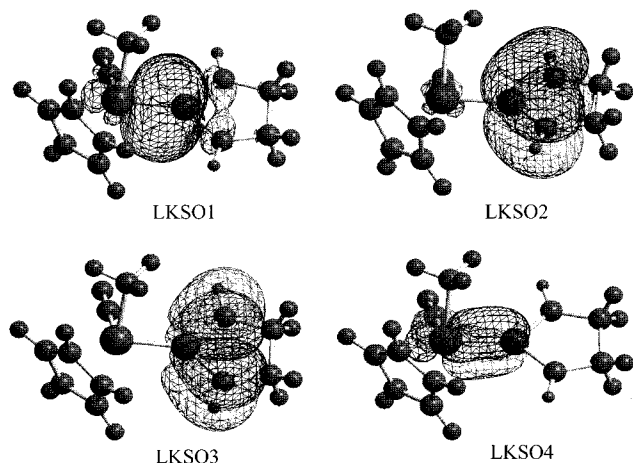
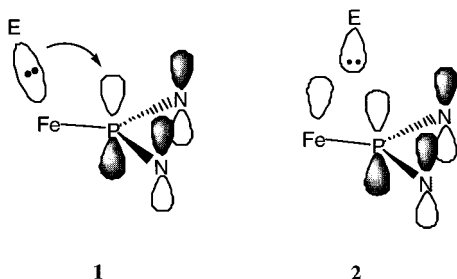


**Figure 4.** Some localized Kohn–Sham orbitals (LKSOs) of the cationic phosphonium–iron complex Cp(CO)(CH<sub>3</sub>)–Fe{[PNHCH<sub>2</sub>CH<sub>2</sub>NH]}<sup>+</sup>.

**(b) Geometries of Transition States.** The present reactions are formally the migration of a group to the vacant orbital of the phosphonium ligand, which mainly consists of the phosphorus 3p orbital, as shown in **1**. It



has been clarified on the basis of the orbital argument that such a migration is easy, assisted by the three-centered interaction shown in **2**.<sup>26</sup>

In Figure 2, the 1,2-migration of a CH<sub>3</sub> group is depicted. It proceeds with the formation of a three-centered transition state (CH<sub>3</sub>–TS1), as expected, with a very small activation barrier of 1.3 kcal/mol to cross. In this transition state (TS), the Fe–CH<sub>3</sub> bond to be broken is only 1.05 times stretched compared with that in the reactant, and the distance of the forming P–C bond is still 24% longer than the product of this

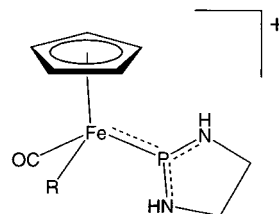


**Figure 5.** Conjugation around the phosphorus atom represented by dotted lines.

elementary step (CH<sub>3</sub>–Intermediate1), indicating that CH<sub>3</sub>–TS1 is an early TS. CH<sub>3</sub>–TS1 leads to the formation of CH<sub>3</sub>–Intermediate wherein the Fe–CH<sub>3</sub> bond is broken completely and the P–CH<sub>3</sub> bond is formed. Interestingly, the intramolecular Fe···CH interaction called an agostic interaction<sup>27</sup> is detected between one of the methyl C–H bonds and the Fe atom. The long agostic C–H bond, which is 0.027 Å longer than the other methyl C–H bonds, and the short distance of 2.097 Å between the Fe atom and the agostic H atom suggest strong agostic interaction. Such an interaction could stabilize transient species appearing during reactions as shown previously.<sup>28</sup>

The 1,2-migration completes at the formation of the CH<sub>3</sub>–Intermediate. However, this complex rearranges via the transition state CH<sub>3</sub>–TS2 to a more stable 18-electron species, CH<sub>3</sub>–Complex2, wherein one of the nitrogen lone pairs coordinates to the Fe atom. The structure of CH<sub>3</sub>–TS2 demonstrates that before this TS the Fe–CH agostic interaction is broken and that after passing this TS the Fe–N bond is formed. Thus, this rearrangement is the change of the coordination from the agostic CH bond to the N atom. In addition the CO ligand migrates to the site that was occupied by the agostic CH bond in CH<sub>3</sub>–Intermediate, to prepare the vacant site for the N coordination. CH<sub>3</sub>–Complex2 is 10.9 kcal/mol more stable than CH<sub>3</sub>–Intermediate, indicating that the N coordination is stronger than the agostic interaction. The activation energy of this rearrangement was calculated to be 3.6 kcal/mol, which is slightly larger than the activation energy of the first step. Since the activation energies of both steps are small, the CH<sub>3</sub> migration is quite easy.

(27) Brookhart, M.; Green, M. L. H. *J. Organomet. Chem.* **1983**, 250, 395, and references therein.

(28) (a) Koga, N.; Obara, S.; Kitaura, K.; Morokuma, K. *J. Am. Chem. Soc.* **1985**, 107, 7109. (b) Koga, N.; Obara, S.; Morokuma, K. *J. Am. Chem. Soc.* **1984**, 106, 4625. (c) Obara, S.; Koga, N.; Morokuma, K. *J. Organomet. Chem.* **1984**, 270, C33.

(26) (a) Woodward, R. B.; Hoffmann, R. *The Conservation of Orbital Symmetry*; Verlag Chemie: Weinheim, 1970. (b) Fukui, K. *Acc. Chem. Res.* **1971**, 4, 57.

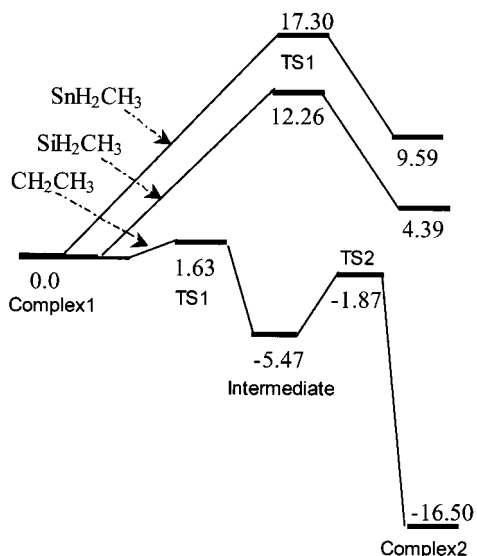


**Figure 6.** Energy profile in kcal/mol for the 1,2-migrations of  $\text{CH}_2\text{CH}_3$ ,  $\text{SiH}_2\text{CH}_3$ , and  $\text{SnH}_2\text{CH}_3$  groups from Fe to P.

$\text{CH}_3$ -TS2 without the agostic interaction or the N coordination has a "classical" structure. As a matter of fact, Nakazawa et al. have showed in their proposed general mechanism<sup>6</sup> that a possible product has a structure similar to  $\text{CH}_3$ -TS2 without the coordination of the N atom. The inability to detect  $\text{CH}_3$ -Complex2 in the experimental conditions could be ascribed to the coordination of other species such as  $\text{BF}_2\text{OCH}_3$  present in the medium to the Fe atom,<sup>6</sup> because it hinders the bond formation between the Fe and N atoms.

On the other hand, the  $\text{SiH}_3$  and  $\text{SnH}_3$  1,2-migrations adopt a one-step mechanism without an intermediate (cf. Figure 3), different from the  $\text{CH}_3$  migration. The structures very similar to  $\text{CH}_3$ -Intermediate were located as a TS as shown in Figure 3; while  $\angle\text{Fe-P-CH}_3$  in  $\text{CH}_3$ -Intermediate is  $74.0^\circ$ ,  $\angle\text{Fe-P-SiH}_3$  in  $\text{SiH}_3$ -TS1 and  $\angle\text{Fe-P-SnH}_3$  in  $\text{SnH}_3$ -TS1 are  $72.4^\circ$

and  $74.0^\circ$ , respectively. The P-Si bond distance of  $2.424 \text{ \AA}$  and the P-Sn bond distance of  $2.681 \text{ \AA}$  are only 4.5 and 2.1%, respectively, longer than those in the products, indicating that in these TSs the P-Si and P-Sn bonds are almost formed, similar to the P-C bond in  $\text{CH}_3$ -Intermediate. These TSs are also characterized by the presence of SiH and SnH agostic interactions, as is evident in their short  $\text{Fe}\cdots\text{HSiH}_2$  and  $\text{Fe}\cdots\text{HSnH}_2$  distances of  $2.297$  and  $2.335 \text{ \AA}$  and the agostic H-Si and H-Sn bonds, which are longer by  $0.026$  and  $0.036 \text{ \AA}$ .

The energy profiles for both the  $\text{SiH}_3$  and  $\text{SnH}_3$  1,2-migrations shown in Figure 3 demonstrate much higher activation barrier of  $19.2$  and  $15.0 \text{ kcal/mol}$ , respectively. Endothermicity of the  $\text{SiH}_3$  and  $\text{SnH}_3$  migrations may result in the larger activation energies, although the agostic interactions stabilize the TS structures for the  $\text{SiH}_3$  and  $\text{SnH}_3$  migrations. The weak P-Si and P-Sn bonds (vide infra) shift up  $\text{SiH}_3$ - and  $\text{SnH}_3$ -TS1 in energy on the potential energy surface to make such structures the TSs, whereas due to the stronger P-C bond,  $\text{CH}_3$ -Intermediate, having a similar structure, is an equilibrium structure.

**1,2-Migration of  $\text{EH}_2\text{CH}_3$  (E = C, Si, and Sn).** Though there are quantitative differences among the  $\text{CH}_3$ ,  $\text{SiH}_3$ , and  $\text{SnH}_3$  migrations, the activation energies of these 1,2-migrations are not too high. This is not consistent with the experimental findings by Nakazawa et al. that 1,2-migration is not observed in the cases of  $\text{Si}(\text{CH}_3)_3$  and  $\text{Sn}(\text{CH}_3)_3$  as a migrating group.<sup>6</sup> Therefore, we studied at the B3LYP/LANL2DZ and B3LYP/LANL2DZ+pol levels the reactions with more realistic migrating groups of  $\text{EH}_2\text{CH}_3$  (E = C, Si, and Sn).

These 1,2-migrations were found to be similar to the corresponding  $\text{CH}_3$ ,  $\text{SiH}_3$ , and  $\text{SnH}_3$  migrations mentioned above (cf. Figure 6). The  $\text{CH}_2\text{CH}_3$  migration passes through an intermediate similar to  $\text{CH}_3$ -Intermediate, and the other migrations for E = Si and E = Sn adopt a one-step mechanism. As compared to

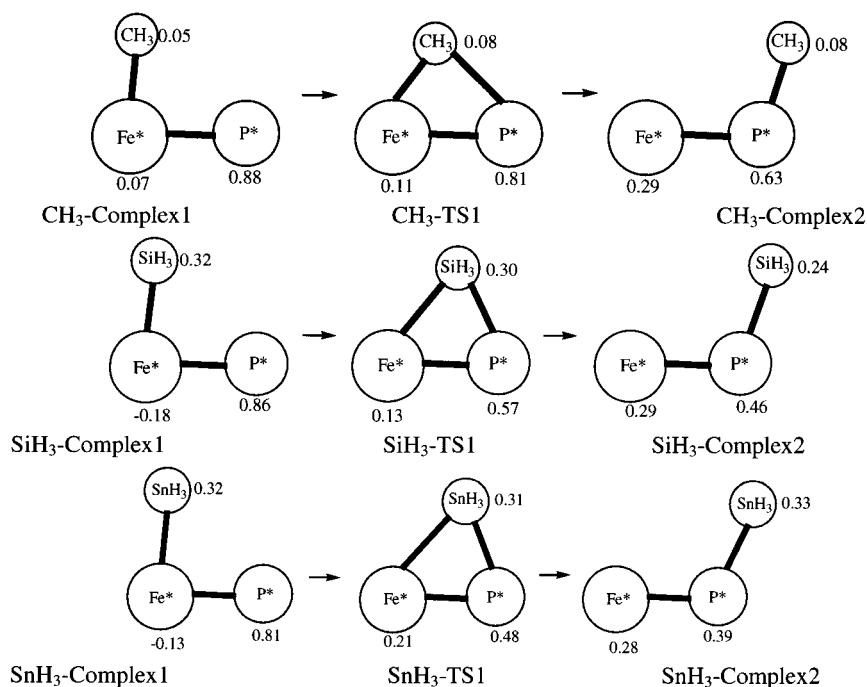


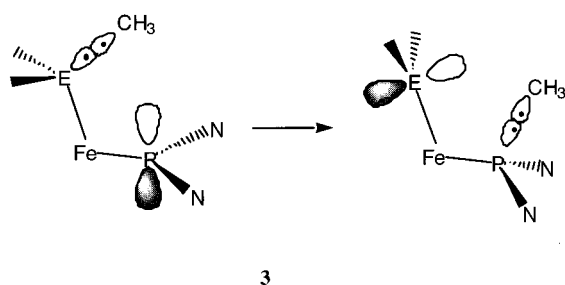
**Figure 7.** Charge reorganizations during the 1,2-migrations.

the 1,2-migrations of  $\text{EH}_3$ , noticeable changes are a small decrease in the activation barriers by 1.9 and 2.7 kcal/mol when  $\text{E} = \text{Si}$  and  $\text{Sn}$ , respectively, and the stabilization of the products by around 2–3.3 kcal/mol. In other words, the methyl substitution on an  $\text{EH}_3$  group slightly enhances the chance of the migration from the Fe atom to the P atom. The electron-donating methyl group enhances the three-centered interaction, **2**, to result in the lower activation energies.

**Analysis of Charge Distribution.** To analyze the charge reorganizations during the 1,2-migrations for  $\text{EH}_3$  groups, cations involved in the reactions have been partitioned into three fragments, viz., the migrating

group, the phosphonium fragment ( $\text{PNHCH}_2\text{CH}_2\text{NH}$ , designated here as  $\text{P}^*$ ), and the rest as the iron fragment ( $\text{Fe}^*$ ). For each partition, the Mulliken charges were calculated, and the results are depicted in Figure 7. From the charge on each fragment, the  $\text{CH}_3$  migration can be easily distinguished from other migrations by the following factors. First, the  $\text{CH}_3$  group shows very small positive charge (nearly zero) as compared to the  $\text{SiH}_3$  and  $\text{SnH}_3$  groups. The second factor is the change in the values of the charges on  $\text{Fe}^*$  and  $\text{P}^*$  as one goes from the reactant to the product. In the  $\text{SiH}_3$  and  $\text{SnH}_3$  migrations, the changes are much larger than that in the  $\text{CH}_3$  migration. The first factor suggests that the Coulombic repulsion between the migrating group and the phosphonium moiety ( $\text{P}^*$ ) is a minimum in the  $\text{CH}_3$  migration and that it could play an important role in deciding the feasibility of other 1,2-migrations. Similar results were obtained for the  $\text{EH}_2\text{CH}_3$  groups as well. An interesting linear correlation between the charge on the phosphonium fragment of all the TSs and the activation energies of the respective reactions (cf. Figure 8) is also obtained. Charges obtained by natural population analysis showed the same kind of linear correlation. Such correlation suggests that the potential energy surface for a 1,2-migration is very sensitive to the charge reorganization during the reaction, and therefore it can be greatly influenced by the external medium such as polar solvent or a counteranion.

**1,3-Methyl Migrations from  $\text{EH}_2$  ( $\text{E} = \text{C}, \text{Si},$  and  $\text{Sn}$ ).** The phosphonium cation as well as silylene and stannylyene isoelectronic to singlet carbene.<sup>7</sup> Accordingly, the 1,3-methyl migration can be formulated by **3**. The migration to the vacant orbital of the phosphonium cation leads to the formation of the vacant p orbital on E.



Therefore, the electronic structures of carbene, silylene, and stannylyene bonds with the Fe atom would affect the reactivity of the complex. The transition metal complexes with such ligands are usually classified into Schrock-type with covalent  $\sigma$  and  $\pi$  bonds and Fischer-

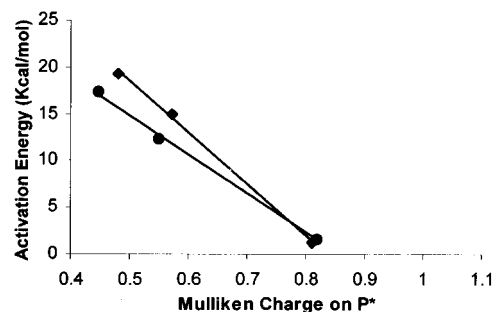
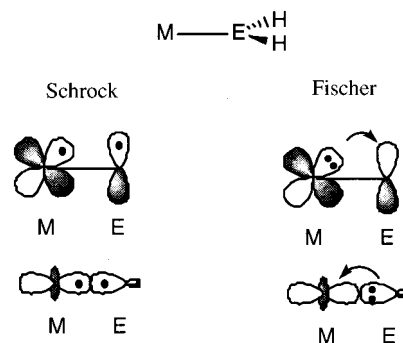
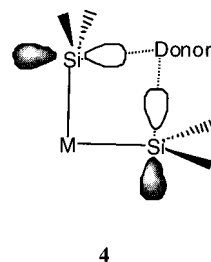


**Figure 8.** The relation between the Mulliken charge on the phosphonium fragment ( $\text{P}^*$ ) in the TS (square for  $\text{EH}_3$ -TS1 and circles for  $\text{EH}_2\text{CH}_3$ -TS1,  $\text{E} = \text{C}, \text{Si},$  and  $\text{Sn}$ ) and the activation energies of the 1,2-migration reactions.

type with donor-acceptor  $\sigma$  and  $\pi$  bonds as shown below.<sup>29</sup>



Previous theoretical studies have shown that, while the methylene complexes adopt the Schrock-type bonds, the silylene complexes are of the Fischer-type,<sup>29,30</sup> because the ground states of methylene and silylene are  $^3\text{B}_1$  and  $^1\text{A}_1$ , respectively. Stannylyene complexes are reasonably considered to be similar to silylene complexes. Recently, donor-bridged bis(silylene) complexes, **4**, have been reported.<sup>31</sup> Such complexes are electronically similar to the TS expected for 1,3-migrations, suggesting that 1,3-migration would be an easy process.



The present calculations have shown that in all the 1,3-migrations we studied, a methyl group bonded to the C, Si, or Sn atom migrates to the P atom through a four-centered TS. In Figure 9, for instance, the structures of the reactant, TS, and product of the 1,3-migration from  $\text{SnH}_2$  are shown along with the energy profiles of the 1,3-migrations from  $\text{EH}_2$  ( $\text{E} = \text{C}, \text{Si},$  and

(29) Arnold, F. P. *Organometallics* **1999**, *18*, 4800.

(30) (a) Koga, N.; Morokuma, K. *J. Am. Chem. Soc.* **1993**, *115*, 6883.

(b) Sakaki, S.; Kai, S.; Sugimoto, M. *Organometallics* **1999**, *18*, 4825, and references therein.

(31) (a) Ueno, K.; Masuko, A.; Ogino, H. *Organometallics* **1997**, *16*, 5023. (b) Ueno, K.; Masuko, A.; Ogino, H. *Organometallics* **1999**, *18*, 2694, and references therein.

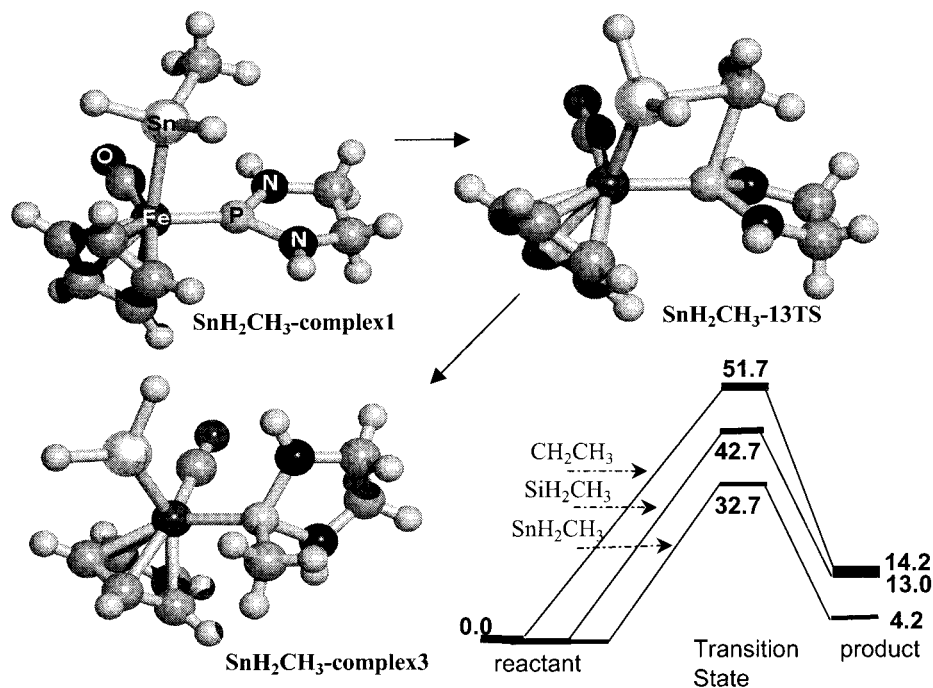


**Figure 9.** 1,3-Migration of the  $\text{CH}_3$  group from  $\text{SnH}_2$  to P. Also shown is the energy level diagram in kcal/mol for the 1,3-migrations of the  $\text{CH}_3$  group from  $\text{CH}_2$ ,  $\text{SiH}_2$ , and  $\text{SnH}_2$  to P. C and H atoms are not labeled.

**Table 2. Important Bond Length Parameters (in Å) in 1,3- $\text{CH}_3$  Migrations Involving the Breaking of the  $\text{EH}_2\text{-CH}_3$  Bond (E = C, Si, and Sn)**

B3LYP/LanL2DZ+pol	Fe-P	Fe-E	P-E	P-N1 <sup>a</sup>	P-N2	E-C
$\text{CH}_2\text{CH}_3\text{-Complex1}$	2.067	2.103	no bond	1.664	1.667	1.536
$\text{CH}_2\text{CH}_3\text{-TS}$	2.137	1.922	2.166	1.677	1.679	2.135
$\text{CH}_2\text{CH}_3\text{-Complex3}$	2.237	1.777	1.854	1.696	1.703	no bond
$\text{SiH}_2\text{CH}_3\text{-Complex1}$	2.053	2.402	no bond	1.665	1.667	1.888
$\text{SiH}_2\text{CH}_3\text{-TS}$	2.151	2.228	2.181	1.678	1.681	2.274
$\text{SiH}_2\text{CH}_3\text{-Complex3}$	2.237	2.146	1.858	1.698	1.709	no bond
$\text{SnH}_2\text{CH}_3\text{-Complex1}$	2.053	2.660	no bond	1.668	1.668	2.141
$\text{SnH}_2\text{CH}_3\text{-TS}$	2.146	2.503	2.361	1.673	1.674	2.438
$\text{SnH}_2\text{CH}_3\text{-Complex3}$	2.237	2.415	1.861	1.700	1.712	no bond

<sup>a</sup> Nitrogen atom nearer to the carbonyl group is designated as N1 and the other as N2.

Sn). In Table 2 selected bond lengths of the stationary points are summarized.

In the products the Fe atom satisfies the 18-electron rule without the N coordination, different from the 1,2-migration reactions, and therefore the reaction terminates with just the 1,3-migration of the  $\text{CH}_3$  group. During the reactions the Fe-E bonds are shortened, because of the double-bond character of the  $\text{M}=\text{E}$  bond in the product as well as the change of hybridization on the E atom. The hybridization of the E atom changes from  $\text{sp}^3$  to  $\text{sp}^2$ , as reflected in the planar structures in the products (sum of the angles around E is  $360^\circ$ ) as well as in the TSs (sum of the angles around E = C, Si, and Sn are  $354.2^\circ$ ,  $355.9^\circ$ , and  $357.6^\circ$ , respectively). The Fe-C bond is shortened by 15.5%, whereas the Fe-Si and Fe-Sn bonds are shortened by only 10.7 and 9.2%, respectively, suggesting the stronger double-bond character of the Schrock-type methylene complex. This is also reflected by the difference in the  $\text{M}=\text{E}$  double bond energies shown later. On the other hand, similar to the changes in the 1,2-migrations, the Fe-P and P-N bonds become longer because of the breaking of the lone-pair  $\pi$  conjugation and the Fe-P  $\pi$  bond.

The activation energies for the  $\text{CH}_3$  1,3-migration from  $\text{CH}_2$  and  $\text{SiH}_2$  were calculated to be 51.7 and 42.7

kcal/mol, respectively. These high activation energies suggest that these reactions are quite unlikely to happen. However, a moderate barrier of 32.7 kcal/mol for the migration from  $\text{SnH}_2$  shows the possibility of this reaction. One of the reasons for this difference comes from the difference in the energy of reaction. The migration from  $\text{SnH}_2$  is less endothermic by 9–10 kcal/mol than the other reactions. The relatively long distance of the C-C bond at the TS is also responsible for the larger activation energy for the reaction from  $\text{CH}_2$ . At the TSs the  $\text{CH}_2\text{-CH}_3$ ,  $\text{SiH}_2\text{-CH}_3$ , and  $\text{SnH}_2\text{-CH}_3$  bonds were stretched so that the  $\text{CH}_3\cdots\text{P}$  interaction necessary for 1,3-migration is achieved. These bonds at the TSs are in fact 1.39, 1.20, and 1.14 times longer than those in the reactants, respectively. As seen in Figure 10, these ratios correlate well with the activation energies.

**Bond Strength Analysis.** The energies of the reactions and activation energies for 1,2- and 1,3-migrations are dependent on the E atom. The  $\text{CH}_3$  1,2-migrations are much easier than the  $\text{SiH}_3$  and  $\text{SnH}_3$  1,2-migrations, whereas the  $\text{CH}_3$  1,3-migration from  $\text{SnH}_2$  is much easier than those from  $\text{SiH}_2$  and  $\text{CH}_2$ . Since the activation energies correlate with the energies of reactions, it is important to investigate the difference in the



Scheme 2

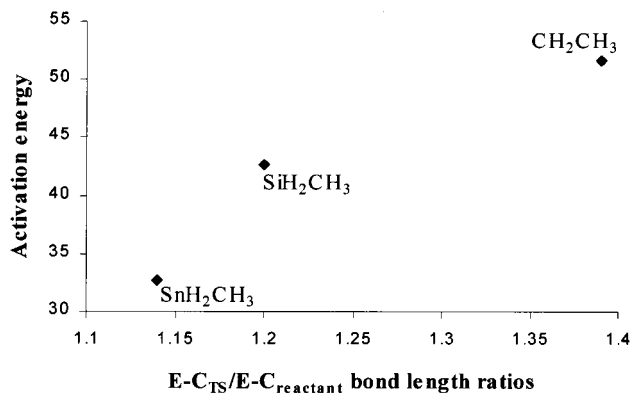
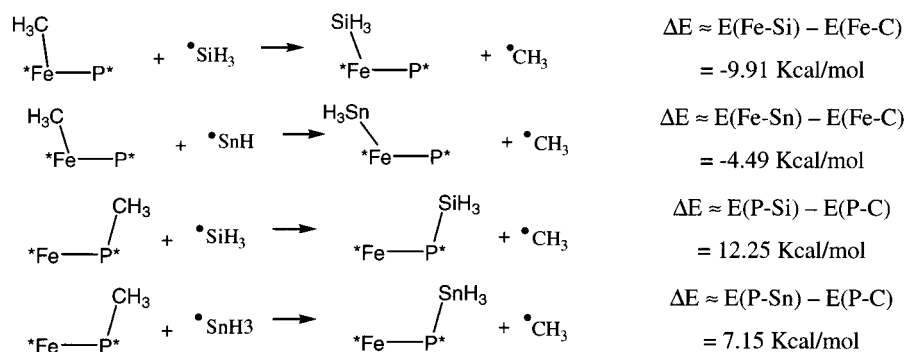


**Figure 10.** Correlation between the activation energies (in kcal/mol) of CH<sub>3</sub> 1,3-migration reactions and the E-C<sub>TS</sub>/E-C<sub>reactant</sub> bond length ratios (E = C, Si, and Sn).

energies of reactions. In this section we analyze the energies of reactions in terms of the strength of the bonds that are formed and broken during the course of the reactions.

In the 1,2-migration reactions, mainly a P-E bond is formed at the expense of an Fe-E bond, where E is C, Si, and Sn. The relative bond strengths can be obtained considering the replacement reactions shown in Scheme 2 because the energy contributions due to the bonds other than the P-E and Fe-E bonds are canceled from both sides of the reactions. The calculations showed that the bond strengths are in the order Fe-Si > Fe-Sn > Fe-C and P-Sn < P-Si < P-C. Quantitative values for the bond strengths of the bonds directly involved in the 1,2- and 1,3-migrations can be obtained in the following way.

It is found that CH<sub>3</sub>-Complex1 and CH<sub>3</sub>-TS2 in the CH<sub>3</sub> 1,2-migration have almost the same energy. As we mentioned, in CH<sub>3</sub>-TS2 neither agostic interaction nor N coordination takes place, and the P-C bond is completely formed. As a consequence, we can say that the energy required in the breaking of the Fe-C bond, the Fe-P π bond, and the N-P<sup>+</sup>-N lone pair π-conjugation in CH<sub>3</sub>-Complex1 is equal to the energy released in the formation of the P-C bond. Let  $E_{\text{conj}}$  stand for the energy required by breaking the Fe-P π bond and the N-P<sup>+</sup>-N lone pair π-conjugation. Then we get eq 1.

$$E_{\text{P-C}} \approx E_{\text{Fe-C}} + E_{\text{conj}} \quad (1)$$

where  $E_{\text{P-C}}$  and  $E_{\text{Fe-C}}$  are the energy released in the formation of the P-C and Fe-C bonds. Accordingly, the

difference in the bond strengths between the P-C and Fe-C bonds can be obtained with  $E_{\text{conj}}$ .  $E_{\text{conj}}$  can be calculated by the energy of an isodesmic reaction<sup>22,32</sup> shown in Figure 11a, and we obtained at the B3LYP/LANL2DZ+pol level  $E_{\text{conj}} = -61.9$  kcal/mol. The energy released in the formation of the P-C bond,  $E_{\text{P-C}}$ , was calculated using the fragmentation reaction shown in Figure 11b to obtain an  $E_{\text{P-C}}$  of -93.7 kcal/mol. Using  $E_{\text{conj}}$ ,  $E_{\text{P-C}}$ , and  $\Delta E$ 's in Scheme 2 as well as the relation in eq 1, we obtained the following values:  $E_{\text{Fe-C}} = -31.8$  kcal/mol,  $E_{\text{Fe-Si}} = -41.7$  kcal/mol,  $E_{\text{Fe-Sn}} = -36.3$  kcal/mol,  $E_{\text{P-Si}} = -81.4$  kcal/mol, and  $E_{\text{P-Sn}} = -72.1$  kcal/mol.

During the 1,3-migrations the E-C bond and conjugation around the P atom are broken, the P-C bond is formed, and the Fe-E single bonds change into the Fe=E double bond. The energies of reactions,  $\Delta E_{1,3}$ , can be written using eq 2.

$$\Delta E_{1,3} = E_{\text{Fe=E}} + E_{\text{P-C}} - E_{\text{Fe-E}} - E_{\text{E-C}} - E_{\text{conj}} \quad (2)$$

We approximated  $E_{\text{E-C}}$  values in eq 2 by those of the H<sub>3</sub>E-CH<sub>3</sub> systems. At the B3LYP/LANL2DZ+pol level we obtained an  $E_{\text{C-C}}$  of -90.4 kcal/mol, an  $E_{\text{Si-C}}$  of -86.6 kcal/mol, and an  $E_{\text{Sn-C}}$  of -69.6 kcal/mol. Using these values as well as the results above, an  $E_{\text{Fe=C}}$  of -77.4 kcal/mol, an  $E_{\text{Fe=Si}}$  of -82.3 kcal/mol, and an  $E_{\text{Fe=Sn}}$  of -69.9 kcal/mol were obtained.

With these results we can account for the difference in the energies of reactions. In the cases of 1,2-migrations, the difference between  $E_{\text{Fe-C}}$  and  $E_{\text{P-C}}$  is 62 kcal/mol, whereas that between  $E_{\text{Fe-Si}}$  and  $E_{\text{P-Si}}$  and that between  $E_{\text{Fe-Sn}}$  and  $E_{\text{P-Sn}}$  are 40 and 36 kcal/mol, respectively, indicating that in the CH<sub>3</sub> 1,2-migration, a stronger P-C bond is formed at the expense of a weaker Fe-C bond, leading to the largest exothermicity. It was shown by theoretical calculations that in the complexes with late transition metals the metal-C bond is weaker than the metal-Si bond, different from the bonds with main element such as P-C and P-Si bonds.<sup>30</sup> This large exothermicity, the weak Fe-C bond, and the features of the charge distributions may result in the small activation for the CH<sub>3</sub> 1,2-migration.

During the course of the CH<sub>3</sub> 1,3-migrations the Fe-C, Fe-Si, and Fe-Sn bonds become stronger by 45, 40, and 34 kcal/mol, respectively. With only these changes in the bond strengths the migration from CH<sub>2</sub> would

(32) (a) Hehre, W. J.; Ditchfield, R.; Radom, L.; Pople, J. A. *J. Am. Chem. Soc.* **1970**, *92*, 4796. (b) Radom, L.; Hehre, W. J.; Pople, J. A. *J. Am. Chem. Soc.* **1971**, *93*, 289.

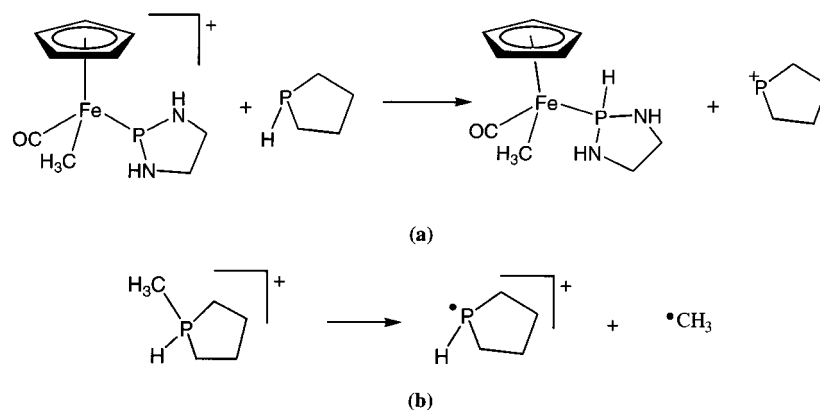


**Figure 11.** (a) Isodesmic reaction used for breaking the conjugation around phosphorus and (b) fragmentation reaction used for calculating the P–C bond energy.

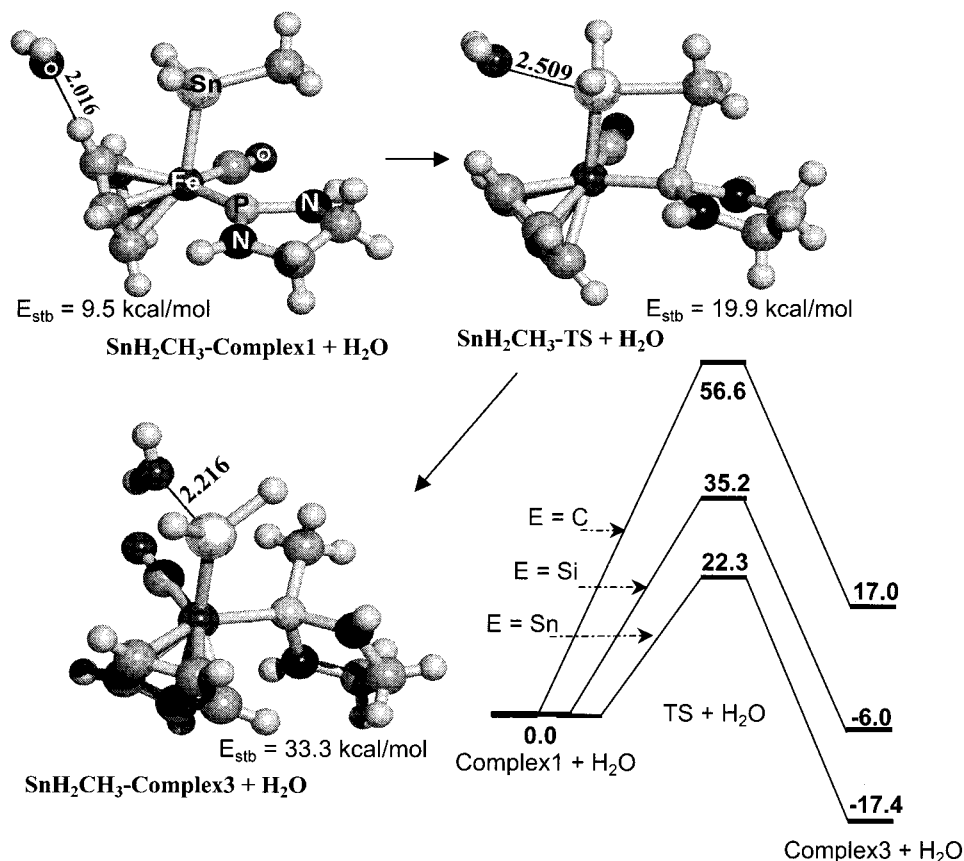


**Figure 12.** H<sub>2</sub>O-mediated 1,3-migration of the CH<sub>3</sub> group from Sn to P (complex–H<sub>2</sub>O stabilization energy,  $E_{\text{stb}}$ , is also shown) and energy level diagram (in kcal/mol) for E = C, Si, and Sn. See text for further details. C and H atoms are not labeled.

be the most exothermic. However, concerning the bonds to be broken, the Sn–C bond is weaker than the C–C and Si–C bonds by 20 and 17 kcal/mol, respectively. This large difference clearly indicates that because of the weak Sn–C bond, the methyl migration from SnH<sub>2</sub> is the least endothermic.

**Effect of Base on 1,3-Migrations: H<sub>2</sub>O-Mediated Reactions.** The above results can account for some of the experimental results. If the ligand is an alkyl group, the alkyl 1,2-migration from Fe to P should be observed, because the calculations showed that the 1,2-migration is more favorable when E = C. Among the 1,3-migrations studied here, only the one involving the breaking of the Sn–C bond was observed in the experiments.

However, the present results show that this reaction is less favorable than the 1,2-migration of the stannyl group, being in disagreement with the experimental result. At this point the experimental finding that the CF<sub>3</sub>SO<sub>3</sub> anion (TfO<sup>−</sup>) promotes the CH<sub>3</sub> 1,3-migration from Sn should be noted.<sup>6</sup> It was also proposed that coordination of the oxygen in TfO<sup>−</sup> to the Sn atom facilitate the reaction. Actually in the X-ray structure of the product for the CH<sub>3</sub> 1,3-migration from the Sn atom, TfO<sup>−</sup> coordinates to the Sn atom. It is therefore expected that the interaction of a base molecule with the E atom of EH<sub>2</sub> would significantly change the energy profile of the 1,3-migrations. To incorporate the coordination effect of a base such as TfO<sup>−</sup>, we have con-

ducted a model study of the 1,3-migrations in the presence of a water molecule, a simple model of base. Since the energetics we have obtained so far at the B3LYP/LANL2DZ and B3LYP/LANL2DZ+pol levels of theory are very similar to each other, we performed the calculations of the H<sub>2</sub>O-mediated reactions only at the B3LYP/LANL2DZ level. We have started geometry determinations with the structures in which a water molecule is initially located near the E atom.

The optimized structures for the CH<sub>3</sub> 1,3-migration from Sn to P are shown in Figure 12. The structures for the 1,3-migrations for E = C and Si are very similar (given in the Supporting Information). Also depicted in Figure 12 is the energy profiles of the reactions with E = C, Si, and Sn. In all the reactants the water molecule is interacting with one of the cyclopentadienyl hydrogen atoms. The corresponding H<sub>2</sub>O...H distance is 2.025, 1.999, and 2.016 Å when E is C, Si, and Sn, respectively. In the TSs the interaction of the water molecule is mainly with the E atom. The distance between the water oxygen atom and the E atom is 2.878, 2.141, and 2.509 Å for E = C, Si, and Sn, respectively. These distances suggest that this interaction is quite strong when the E atom is Si or Sn and somewhat weak when E = C.

The energy profiles of the reactions further support this argument. The stabilization energies ( $E_{\text{stb}}$ ) upon water coordination at the B3LYP/LANL2DZ level are 8.9, 8.1, and 8.6 kcal/mol for the reactant, the TS, and the product for E = C, while they are 9.1, 16.6, and 31.9 kcal/mol for E = Si and 9.5, 19.9, and 33.3 kcal/mol for E = Sn. It is thus obvious that the water mediation has no significant effect on the energy profile when the CH<sub>3</sub> group migrates from C to P and that, on the other hand, the methyl migration from Si to P and that from Sn to P become exothermic with significant changes in the activation barriers as compared to the reactions without water mediation.

How do we explain these differences? A possible reason can be given based on the M=EH<sub>2</sub> bond features mentioned before. Since the Fe=SiH<sub>2</sub> and Fe=SnH<sub>2</sub> complexes are Fischer-type, the electron density of the p orbitals of SiH<sub>2</sub> and SnH<sub>2</sub> fragments is small. Accordingly, the lone pair of the water molecule can interact strongly with the Si and Sn atoms. On the other hand, the p orbital of CH<sub>2</sub> takes part in the Fe=C  $\pi$  bond, and therefore the interaction between water and CH<sub>2</sub> is weaker.

Although the activation energies for E = Si and Sn drastically decrease, even the H<sub>2</sub>O-mediated 1,3-migration with E = Sn has a higher activation barrier than the corresponding 1,2-migration, different from the experimental observation. However, we note that the effect of base is only partially accounted in the model calculations, and in the actual situation a negative base (TfO<sup>-</sup>) could coordinate much more strongly than water, and thus the effect is probably larger. With TfO<sup>-</sup> the activation energy of 1,3-migration is expected to be smaller than that of 1,2-migration.

### Concluding Remarks

All the tricoordinated phosphonium iron complexes studied in the present work show N–P<sup>+</sup>–N lone pair  $\pi$ -conjugation. Further, this conjugation is extended to

the metal atom via an Fe–P<sup>+</sup>  $\pi$  bond. Both together contribute 61.9 kcal/mol toward the stability of these cationic species. In such a complex, a 1,2-migration of a methyl or ethyl group from iron to phosphorus is highly favored due to the very small activation energies needed by the reaction. A weak Fe–C bond in the reactant and the large exothermicity, which can be explained from the strong P–C bond formed in the product, account for this small activation barrier. The small charge on the methyl group is an additional advantage for this reaction because it reduces the opposing Coulombic repulsion between the migrating group and the phosphonium cation moiety. Different from 1,2-methyl migration, 1,2-silyl and 1,2-stanny migration are endothermic reactions, and they need larger activation energies. This happens because the Fe–Si and Fe–Sn bonds that are broken in the reactant are stronger than the Fe–C bond, and the P–Si and P–Sn bonds that are formed in the product are not as strong as a P–C bond. Another disadvantage of 1,2-silyl and 1,2-stanny migrations is the larger Coulombic repulsion between the migrating group and the cationic phosphonium moiety as compared to the that for the 1,2-methyl migration. The linear correlation between the activation energy and the net charge on the phosphonium moiety in the transition state for the 1,2-migrations suggests that these reactions are very sensitive to the charge reorganization during the migration process. Therefore, the solvent as well as the counterions may also play an important role in deciding the courses of these reactions.

In 1,3-migrations, essentially C–CH<sub>3</sub>, Si–CH<sub>3</sub>, and Sn–CH<sub>3</sub>  $\sigma$  bonds are broken. Their bond strengths are in the order C–CH<sub>3</sub> > Si–CH<sub>3</sub> > Sn–CH<sub>3</sub>. A weak and long Sn–CH<sub>3</sub> bond results in the easier formation of a four-centered transition state for the 1,3-methyl migration from tin to phosphorus as compared to other 1,3-migrations. Unlike 1,2-migrations, 1,3-migrations have no correlation between charge on any of the fragments and the activation energy. Further, since the migrating group is methyl in all the 1,3-migrations, the Coulombic factor may be almost the same for all these reactions. The effect of a base in the 1,3-migrations is unraveled through the water-mediated reactions. Water mediation makes a significant decrease in the activation barriers of the reactions when E = Si and Sn. Further, the water-mediated 1,3-methyl migrations from Si to P and Sn to P become exothermic, which are not otherwise.

The theoretical results presented here support a very fast 1,2-methyl migration, which is in good agreement with the experimental results obtained by Nakazawa et al.<sup>6,21</sup> The 1,3-methyl migrations involving the cleavage of C–CH<sub>3</sub> and Si–CH<sub>3</sub> are less likely to happen, in agreement with the experiments. Experimental results support only a 1,3-methyl migration from tin to phosphorus, and the present calculations showed that base could play a critical role to realize this migration. One intriguing result in the experiment is the absence of any migration product when E = Si. However, the theoretical results presented here are in favor of a 1,2-migration.

In fact, several general issues regarding structural, energetic, and bonding features of the complexes as well as more specific issues regarding migration reactions

are described herein. These include lone pair conjugation, orbital interaction, agostic interaction, charge reorganization during the course of a reaction, solvent effect, and bond energy calculations. Moreover, the importance of the formation of Fischer-type and Schrock-type complexes for the 1,3-migration reactions is discussed. It is hoped that the chemistry described herein for the model cationic phosphonium–iron complex could be applicable to any metal–phosphonium complexes as well as related systems such as metal–carbene and metal–silylene complexes.

**Acknowledgment.** We are grateful to Professor H. Nakazawa for suggestions. The research was supported

by the Grant-In Aid for Scientific Research on Priority Areas “Molecular Physical Chemistry” from the Ministry of Education, Culture, Sports, Science, and Technology. Part of the calculations was carried out at the Research Center for Computational Science of Okazaki National Research Institutes, Japan. C.H.S. gratefully acknowledge the Japan Society for the Promotion of Science (JSPS) for a fellowship.

**Supporting Information Available:** Figures describing the optimized geometries of the  $\text{EH}_2\text{CH}_3$  1,2-migrations ( $\text{E} = \text{C}, \text{Si}, \text{and Sn}$ ) as well as the  $\text{H}_2\text{O}$ -mediated  $\text{CH}_3$  1,3-migrations from  $\text{CH}_2$  to P and  $\text{SiH}_2$  to P.

OM010402V